Controlled synthesis and characterization of the enhanced local field of octahedral Au nanocrystals†

Jinhwa Heo,[ab] Deok-Soo Kim,[c] Zee Hwan Kim,*[c] Young Wook Lee,[a] Dongheun Kim,[a] Minjung Kim,[a] Kihyun Kwon,[a] Hyung Ju Park,[b] Wan Soo Yun*[b] and Sang Woo Han*[a]

Received (in Cambridge, UK) 11th September 2008, Accepted 16th October 2008
First published as an Advance Article on the web 30th October 2008
DOI: 10.1039/b815925d

Octahedral Au nanocrystals with localized surface plasmon-assisted enhancing optical properties can be prepared in aqueous solution *via* the forced reduction of Au ions by ascorbic acid through the addition of NaOH.

The physicochemical properties of metal nanoparticles critically depend on their size and shape, which can benefit a variety of optical and catalytic applications. Therefore, it is important to develop synthetic methods that can control the morphology and size of the nanoparticles.[1–3] Noble metal nanoparticles also exhibit a surface-enhanced Raman scattering (SERS) activity in which the scattering cross-sections are dramatically enhanced for molecules adsorbed thereon, and this SERS property is highly sensitive to the shape and size of nanoparticles.[4,5] In particular, polyhedral Au nanoparticles show efficient SERS activities and give much stronger signals than do spherical particles.[6,7] The enhanced SERS activity of polyhedral particles is mainly due to their morphological characteristics: they have more well-defined edges and corners, and have generally sharper surface features than do spheres, facilitating the induction of greater localized field enhancement.[6] Accordingly, there is a strong interest in the preparation of polyhedral noble metal nanoparticles with tailored shape and size for realizing their practical applications.[8–12]

Here we report an efficient room-temperature aqueous-phase synthesis of crystalline Au nanoparticles with octahedral shape. To date, several synthesis method have been reported for the preparation of octahedral Au nanoparticles including modified polyol processes,[13,14] thermal decomposition of metal precursors in polymer matrix,[7] and ultrasound-induced reduction.[15] However, most of the previous approaches involved the use of toxic organic solvents or reagents, and required pre-synthesized seeds, high temperature, or prolonged reaction time. The aqueous-phase procedure we have developed in this work does not use such organic reagents, seeds, or foreign metal ions, therefore it is more convenient and environment-friendly than the previous synthesis protocols.[16] Furthermore, we have found that the prepared particles show efficient SERS properties, which can be attributed to the strong field localization at the vertices of the octahedra. Such field localization was confirmed by the scattering-type apertureless near-field scanning optical microscopy (ANSOM)[17–19] measurements.

Octahedral Au nanoparticles were synthesized at room temperature (25 °C) simply by mixing an aqueous solution of $HAuCl_4$, cetyltrimethylammonium bromide (CTAB), and ascorbic acid, followed by the addition of NaOH to induce the nanoparticle formation. In a typical synthesis, to a 20 mL aqueous solution of $HAuCl_4$ (1.25×10^{-4} M) and CTAB (10 mM) was added 100 μL of 100 mM ascorbic acid. Due to its weak reducing strength, ascorbic acid is ineffective in reducing Au(III) to Au(0).[20–22] The light yellow color of the Au salt–CTAB mixture changed to colorless when ascorbic acid was added, indicating the reduction of Au(III) to Au(I). Au hydrosol with purple–red color was formed within 20 min after the injection of NaOH (100 mM, 100 μL) to this reaction mixture (see inset of Fig. 1). The UV-Vis extinction spectrum of the prepared hydrosol exhibits a single strong surface plasmon peak at 547 nm which can be assigned to dipole plasmon resonance (Fig. 1),[13,14] demonstrating that the addition of NaOH leads to the formation of Au nanoparticles. The forced reduction of Au ions by ascorbic acid through the addition of NaOH has been reported to be important in the kinetically controlled formation of nanocrystals with well-defined shapes.[21,22]

Fig. 2(a) shows a representative scanning electron microscopy (SEM) image of the product, which demonstrates that

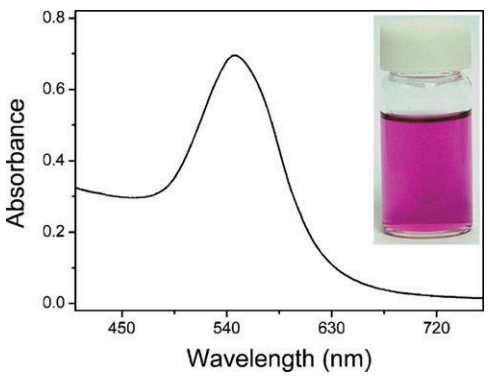

Fig. 1 UV-Vis extinction spectrum of the octahedral Au nanoparticles. The inset shows a digital picture of the aqueous solution of the octahedral Au nanoparticles.

[a] *Department of Chemistry, Research Institute of Natural Science, and Environmental Biotechnology National Core Research Center, Gyeongsang National University, 660-701 Jinju, Korea. E-mail: swhan@gnu.ac.kr*
[b] *Division of Advanced Technology, Korea Research Institute of Standards and Science, Daejeon, 305-600, Korea. E-mail: wsyun@kriss.re.kr*
[c] *Department of Chemistry, Korea University, Seoul, 136-701, Korea. E-mail: zhkim@korea.ac.kr*

† Electronic supplementary information (ESI) available: Details for synthesis and characterization, and additional experimental data. See DOI: 10.1039/b815925d

the majority (>85%) of the sample was octahedral nanoparticles with mean edge length of 38 ± 2 nm. The X-ray diffraction (XRD) pattern of the prepared sample revealed that the nanoparticles are pure crystalline face-centered cubic (fcc) Au (Fig. S1, ESI†). Fig. 2(b) shows a high-resolution transmission electron microscopy (HRTEM) image of a typical octahedral Au nanoparticle. The selected area fast Fourier transform (FFT) pattern obtained from one of the faces of a particle is also shown in the inset. The observed spots with hexagonal symmetry can be assigned to the (220) reflections of the fcc Au crystal, which is characteristic of a single crystalline Au nanocrystal bounded by {111} basal planes.[7,13] The enlarged image of Fig. 2(b) further confirmed the exposed surface of {111} face (Fig. 2(c)); a *d*-spacing of 2.35 Å for adjacent lattice planes corresponds to the {111} planes of fcc Au.[6]

In general, the shape of noble metal nanoparticles can be controlled by manipulating the metal precursor reduction kinetics and the surface growth rates through the specific adsorption of surfactants, stabilizers, and ions.[8–14] In our experimental condition, the formation of Au octahedra can be ascribed to the result of a fast nucleation/growth process.[12] When the reduction rate of Au precursor was decreased by reducing the amount of NaOH, other shapes (mostly cuboctahedra or cubes) with large particle size were produced. Fig. 3 shows SEM images of Au nanoparticles prepared with 50 and 30 mM NaOH solutions under otherwise identical synthetic conditions. With reduced amount of NaOH, the reaction time was increased to about 3 h. As the reduction rate decreased, the shape of nanoparticles changed from octahedra (Fig. 2(a)) to cuboctahedra (Fig. 3(a)) and finally cubes (Fig. 3(b)). The mean edge lengths of cuboctahedra and cubes are 72 ± 3 and

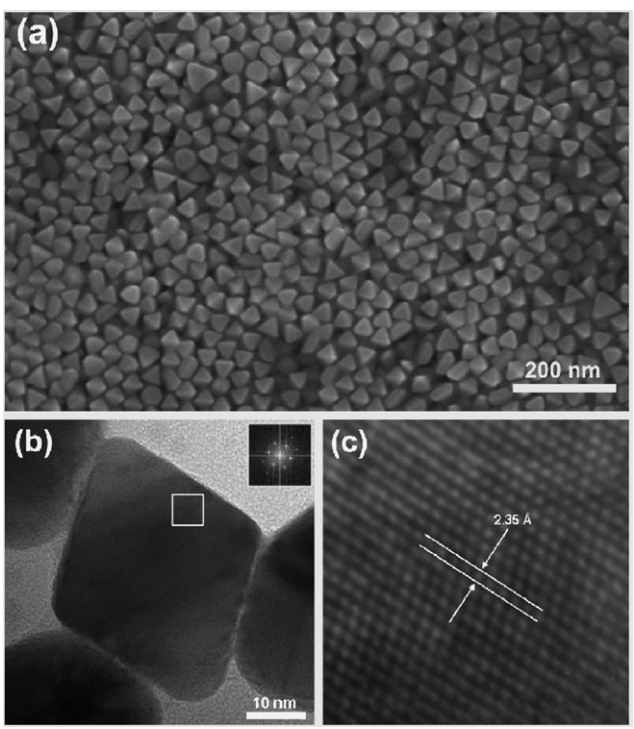

Fig. 2 (a) SEM and (b) HRTEM images of octahedral Au nanoparticles. The inset in (b) shows the selected area FFT pattern. (c) Enlarged image of the square region in (b).

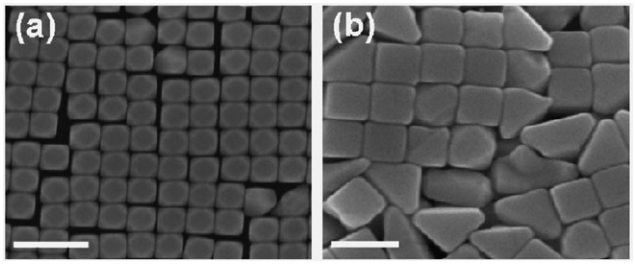

Fig. 3 SEM images of Au nanoparticles prepared with (a) 50 and (b) 30 mM NaOH solution. The scale bars represent 200 nm for each image.

122 ± 9 nm, respectively. This observation indicates that a slow nucleation/growth process facilitates the thermodynamic growth of {111} over {100} facet, producing large cuboctahedra or cubes.[23] We believe that CTAB is crucial for the formation of polyhedral particles because roughly spherical particles were obtained in the absence of CTAB in the reaction mixture (Fig. S2, ESI†). The detailed studies on the mechanism of the formation of polyhedral particles including the exact role of CTAB are currently underway.

The SERS activity of the Au octahedra was investigated to examine the plasmonic properties of the particles. Fig. 4(a) and (b) show, respectively, normal Raman and SERS spectra of rhodamine 6G (R6G) molecules in aqueous solutions obtained with 633 nm excitation. The octahedral Au nanoparticles gave strong SERS signal. The average Raman scattering enhancement factor is estimated to be on the order of 10^6–10^7, which is significantly higher than those for isolated spherical Au nanoparticles (10^3–10^4).[24] We believe that the strong SERS activity of Au octahedra originates from the strongly enhanced field formed at the sharp vertices of the octahedra.[4–6,24]

In order to verify the location of such "hotspots" in the octahedra, ANSOM measurements were carried out. As recently demonstrated, the ANSOM can visualize the plasmonic field distribution around metallic nanostructures by converting the localized near-field into the propagating far-field.[17–19] Briefly, a p-polarized (perpendicular to the sample surface)

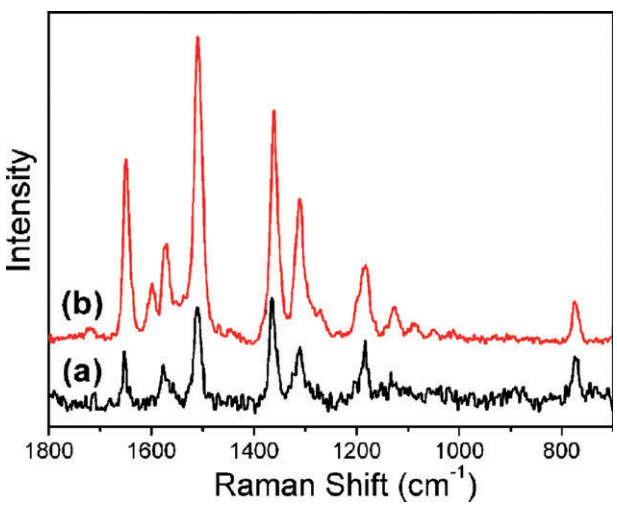

Fig. 4 (a) Normal Raman spectrum of 1 M R6G. (b) SERS spectrum of 5×10^{-7} M R6G obtained with Au octahedra in aqueous solution.

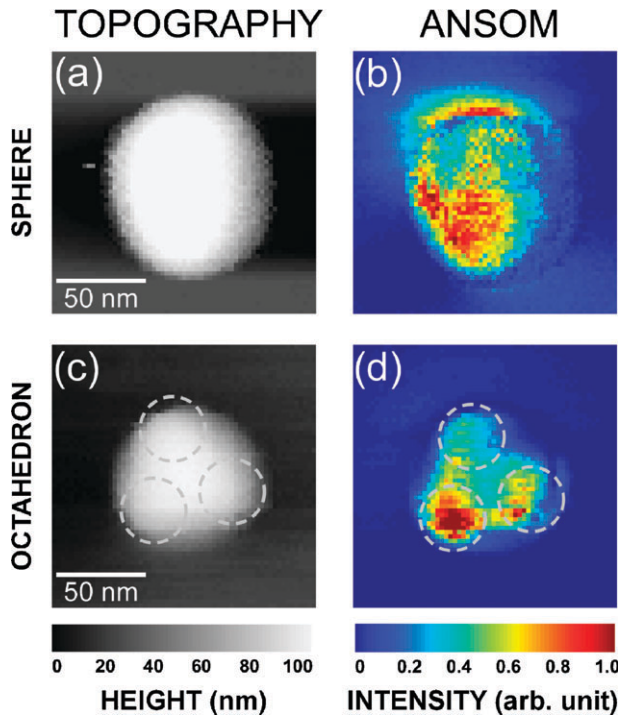

Fig. 5 The topography and ANSOM optical images of an Au nanosphere (a and b) and an Au octahedron (c and d). The dashed circles in (c) and (d) point to the hotspot regions within the nanoparticle.

focused 633 nm laser beam excites the localized field distributions around the nanoparticle and the scanning probe tip serves as a local scatterer of the local field. The scattered light from the tip–sample junction is recorded as a function of tip position above the sample surface (see Fig. S3, ESI†). Fig. 5 displays topography and ANSOM scattering images of an Au sphere (Fig. 5(a) and (b)) and an Au octahedron (Fig. 5(c) and (d)) obtained with the same measurement conditions. The ANSOM image of the sphere exhibits unimodal field distribution at the near-center position of the particle, which is expected from the near-vertically aligned dipole of the sphere.[17] On the other hand, the corresponding ANSOM image of the octahedron shows three distinctly bright spots (dashed circles in Fig. 5) that appear to originate from the vertexes of the top triangular facet of the octahedral nanoparticle, although the atomic force microscopy (AFM) topography can not completely resolve the triangular shape of the top surface of the octahedron (note that the spatial resolution of ANSOM can be better than that of the AFM topography because of the harmonic demodulation process of the optical signal[17–19]). Currently, we are unable to quantify the degrees of enhancements and localizations that occur at the vertexes of the octahedra. However, our ANSOM data of the Au octahedron unambiguously verify the existence of the resonant local fields at the vertices of the octahedron.

In summary, we have presented an aqueous room-temperature synthesis method for the production of octahedral Au nanocrystals. The Au octahedra show localized surface plasmon-assisted enhancing optical properties. Since the synthesized nanoparticles have unique structural and optical properties, they will find applications as materials for the fabrication of novel nanostructures and the optical sensors with high efficiency.

This work was supported by the Korea Research Foundation Grant funded by the Korean Government (MOEHRD) (KRF-2007-313-C00368), by a grant from the MOST/KOSEF to the Environmental Biotechnology National Core Research Center (Grant No. R15-2003-012-01001-0) and to EPB Center (Grant No. R11-2008-052-02003), and by a grant funded by MOST/KOSEF (R01-2008-000-12194-0).

Notes and references

1 C. Burda, X. Chen, R. Narayanan and M. A. El-Sayed, *Chem. Rev.*, 2005, **105**, 1025.
2 Y. Xia and N. J. Halas, *Mater. Res. Soc. Bull.*, 2005, **30**, 338.
3 N. L. Rosi and C. A. Mirkin, *Chem. Rev.*, 2005, **105**, 1547.
4 K. Kneipp, H. Kneipp and J. Kneipp, *Acc. Chem. Res.*, 2006, **39**, 443.
5 C. J. Orendorff, A. Gole, T. K. Sau and C. J. Murphy, *Anal. Chem.*, 2005, **77**, 3261.
6 K. Kwon, K. Y. Lee, Y. W. Lee, M. Kim, J. Heo, S. J. Ahn and S. W. Han, *J. Phys. Chem. C*, 2007, **111**, 1161.
7 J. Zhang, Y. Gao, R. A. Alvarez-Puebla, J. M. Buriak and H. Fenniri, *Adv. Mater. (Weinheim, Ger.)*, 2006, **18**, 3233.
8 T. K. Sau and C. J. Murphy, *J. Am. Chem. Soc.*, 2004, **126**, 8648.
9 F. Kim, S. Connor, H. Song, T. Kuykendall and P. Yang, *Angew. Chem., Int. Ed.*, 2004, **43**, 3673.
10 B. Wiley, Y. Sun, B. Mayers and Y. Xia, *Chem.–Eur. J.*, 2005, **11**, 454.
11 Y. Xiong and Y. Xia, *Adv. Mater. (Weinheim, Ger.)*, 2007, **19**, 3385.
12 A. R. Tao, S. Habas and P. Yang, *Small*, 2008, **4**, 310.
13 C. Li, K. L. Shuford, Q.-H. Park, W. Cai, Y. Li, E. J. Lee and S. O. Cho, *Angew. Chem., Int. Ed.*, 2007, **46**, 3264.
14 D. Seo, J. C. Park and H. Song, *J. Am. Chem. Soc.*, 2006, **128**, 14863.
15 A. Sánchez-Iglesias, I. Pastoriza-Santos, J. Pérez-Juste, B. Rodríguez-González, F. J. García de Abajo and L. M. Liz-Marzán, *Adv. Mater. (Weinheim, Ger.)*, 2006, **18**, 2529.
16 B. Lim, Y. Xiong and Y. Xia, *Angew. Chem., Int. Ed.*, 2007, **46**, 9279.
17 Z. H. Kim and S. R. Leone, *Opt. Express*, 2008, **16**, 1733.
18 R. Hillenbrand, F. Keilmann, P. Hanarp, D. S. Sutherland and J. Aizpurua, *Appl. Phys. Lett.*, 2003, **83**, 368.
19 R. Hillenbrand and F. Keilmann, *Appl. Phys. B: Lasers Opt.*, 2001, **73**, 239.
20 N. R. Jana, L. Gearheart and C. J. Murphy, *Langmuir*, 2001, **17**, 6782.
21 S. Chen, Z. L. Wang, J. Ballato, S. H. Foulger and D. L. Carroll, *J. Am. Chem. Soc.*, 2003, **125**, 16186.
22 C. L. Nehl, H. Liao and J. H. Hafner, *Nano Lett.*, 2006, **6**, 683.
23 C. Wang, H. Daimon, T. Onodera, T. Koda and S. Sun, *Angew. Chem., Int. Ed.*, 2008, **47**, 3588.
24 H. Wang and N. J. Halas, *Adv. Mater. (Weinheim, Ger.)*, 2008, **20**, 82.